Instruction of the CADET-SMB

Qiaole HE

June 16, 2016

Contents

1 Introduction

There are various practical modes of carrying out industrial purifications by preparative chromatography. The most straightforward and the frequently used one is the cyclic batch elution chromatography, simulations of that have been provided in the CADET framework (http://github.com/modsim/CADET). Another important mode is the counter-current chromatography, in which the fluid phase and the solid phase flow through the column in opposite directions. Since the continuous true moving bed (TMB) chromatographic processes are technically hard to implement, the periodically simulated moving bed (SMB) chromatographic processes are usually applied. In this documentation, we offer an introduction for the extension of the CADET framework, CADET-SMB, for simulating SMB processes.

1.1 True Moving Bed Chromatography (TMB)

The configuration of TMB consists of a vertical column in which the fluid phase injected upward while the solid phase is poured into the column in the opposite direction (downward in this case). Then a feed solution is continuously injected into the stream of the fluid phase, in the middle of the column. Both components are collected in the opposite outlets.

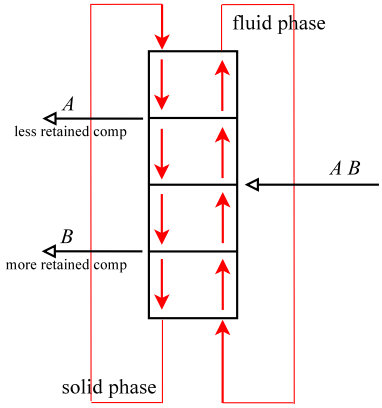

Figure 1: The schematic of the continuous true moving bed (TMB) chromatographic process

The advantages of TMB processes over the traditionally bath elution processes are manifest, especially in terms of the high yields and lower consumptions. However, enormous difficulties have been encountered in the implementation of the TMB process, because it is nearly impossible to achieve the continuous flowing of the fragile solid phase. The practical implementation of the TMB process is the following simulated moving bed (SMB) chromatographic processes.

1.2 Simulated Moving Bed Chromatography (SMB)

The mentioned drawbacks of the TMB processes can be alleviated by replacing the continuous flow of the solid phase by a discontinuous (pseudo-continuous) one. The solid phase does

not actually move, instead it "moves" periodically by switching the inlet and outlet ports, hence the name of this process. It uses a set of shorter columns, instead of a single long column like in the TMB process, connected through complex ports. The attractive point of the SMB process is its efficient use of the solid beads and the yields and purity achieved are often very high. The disadvantage is the waiting time to reach the cyclic steady state (CSS).

A schematic of the SMB process is shown in Fig.(2). In the above unit, there are two

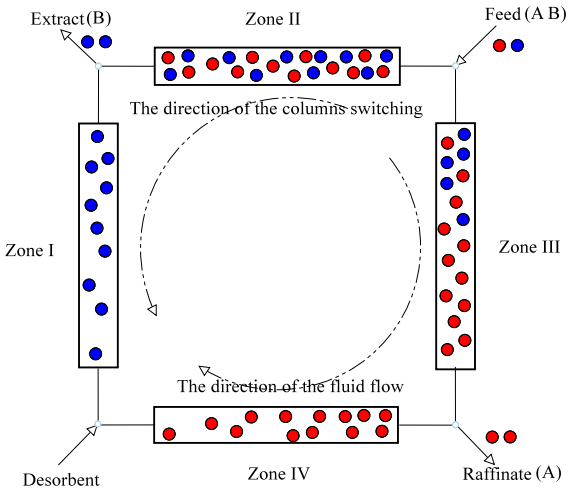

Figure 2: The schematic of the periodically simulated moving bed (SMB) chromatographic process for binary separation

inlet ports, feed and desorbent respectively, and two withdrawal ports, raffinate and extract respectively. The feed buffer is injected into the feed port, while the desorbent in the desorbent port are used for regenerating the columns. The one with lower retention coefficient (less retained) will be withdrawn in the raffinate port while the one with higher retention factor (strong retained) in the extract port.

According to the position of the columns, the unit can be divided into four different zones, each with a specific role in the separation process:

Zone I between the desorbent and the extract ports where the regeneration process of the columns happens and the desorption of the more retained component takes place;

Zone II between the extract and the feed ports where the adsorption of the more retained component takes place;

Zone III between the feed and the raffinate ports where the adsorption of the less retained component takes place;

Zone IV between the raffinate and the desorbent ports the desorption of the less retained component takes place;

Assuming under the proper control of the pump, we have the constant flow rate in different zones. And additionally given the switch time of the SMB unit and column informations, the simulations could be fired up.

2 Mathematical Models

2.1 Column Modelling

Considering the case, N columns of length L are packed with the solid beads of radius r_p. All components are assumed to be homogeneously distributed over the cross-section of interstitial column volume. The bulk mass balance, including convection, dispersion, and film mass transfer, is

$$\frac{\partial c_i^j}{\partial t} = -u_{int}^j \frac{\partial c_i^j}{\partial z} + D_{ax}^j \frac{\partial^2 c_i^j}{\partial z^2} - \frac{1-\varepsilon_c}{\varepsilon_c} \frac{3}{r_p} k_{f,i}^j (c_i^j - c_{p,i}^j), \tag{1}$$

where c_i^j is the interstitial concentration of component i in column j; u_{int}^j is the interstitial velocity in column j; D_{ax}^j is the dispersive coefficient; ε_c is the column porosity (interstitial porosity); $k_{f,i}^j$ is the film mass transfer coefficient; $c_{p,i}^j$ is the mobile phase concentration in the beads; and j represents the column in different zones. Afterwards, the superscript j is omitted for the sake of simplicity. While the bead mass balance, including only diffusion and sorption, is

$$\frac{\partial c_{p,i}}{\partial t} = D_{p,i}\left(\frac{\partial^2 c_{p,i}}{\partial r^2} + \frac{2}{r}\frac{\partial c_{p,i}}{\partial r}\right) - \frac{1-\varepsilon_p}{\varepsilon_p}\frac{\partial q_i}{\partial t}, \tag{2}$$

where $D_{p,i}$ is the pore diffusion coefficient; ε_p is the pore porosity; q_i is the stationary phase concentration in the beads.

In addition, the Danckwerts boundary conditions are required,

$$\begin{cases} \left.\dfrac{\partial c_i}{\partial z}\right|_{z=0} = \dfrac{u_i}{D_{ax}}(c_i(t,0) - c_{in,i}(t)) \\ \left.\dfrac{\partial c_i}{\partial z}\right|_{z=L} = 0 \end{cases} \tag{3}$$

The above model is the general rate model (GRM) which can be simplified into the equilibrium-dispersive model with the linear driving force (LDF) model in the descent manner. Thus the interstitial mass balance model is

$$\frac{\partial c_i}{\partial t} = -u_i \frac{\partial c_i}{\partial z} + D_{ax}\frac{\partial^2 c_i}{\partial z^2} - \frac{1-\varepsilon_t}{\varepsilon_t}\frac{\partial q_i}{\partial t}, \tag{4}$$

while regarding the bead mass balance, the LDF model is used,

$$\frac{\partial q_i}{\partial t} = k_{f,i}\frac{3}{r_p}(c_i - c_{p,i}), \tag{5}$$

where ε_t is the total porosity, and the situation, $D_{ax} = 0$, could be a special case of the equilibrium-dispersive models.

We have implemented the linear kinetic model and competitive Langmuir kinetic model,

$$q_i = H_i c_{p,i} \tag{6}$$

$$q_i = \frac{H_i c_i}{1 + \sum_{i=1}^{N_{comp}} b_j c_j}, \tag{7}$$

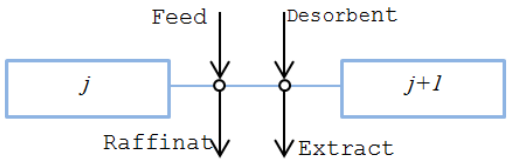

Figure 3: The schematic diagram of two adjacent columns. Note that the adjacent columns here do not have to be *physical* adjacent columns.

where H_i is the Henry's coefficient, b_j is the coefficients related to the adsorption energy.

2.2 Node Balance

In order to complete the model for the SMB process, we have to define the connection of two adjacent columns. Let the inlet concentration of the column j for the component i be denoted by $c_i^{in,j}$, analogously the outlet concentration by $c_i^{out,j}$. Additionally inlets and outlets, like feed, raffinate, desorbent, and extract (extract_1 and extract_2 in ternary situation) will be denoted by scripts F, R, D, and $E(ext\_1, ext\_2)$ respectively. Fig.(3) illustrates the schematic diagram of two adjacent columns j and $j+1$. It is worthy emphasizing that the adjacent columns here do not have to be *physical* adjacent columns, since in the one-column analog it is the column of $(N-1)t_s$ time unit before. Thus the time variable in concentration is omitted here.

For the connecting nodes we obtain the following node balance:

$$c_i^{in,j+1} = \frac{c_i^{out,j} Q_j + \delta}{Q_{j+1}} \tag{8}$$

where the δ varies in different zones due to inlet and outlet ports, and Q_j is the actual volumetric flow rate of mobile phase through column j. It is related to the liquid phase velocity (interstitial velocity) by $Q_j = \varepsilon_t A u_j$, where A is the column cross-section area. Moreover, we do not track the internal composition profile (immediate concentration) in each column of process, instead the outlet concentration, $c_i^{out,j}$, of each column.

$$\delta = \begin{cases} c_F Q_F & F \\ 0 & D \\ c_i^{out,j} Q_R & R \\ c_i^{out,j} Q_E & E\,(binary) \\ c_i^{out,j} Q_{ext} & ext\_1 \quad ext\_2\,(ternary) \end{cases} \tag{9}$$

2.3 Dead Volume Modelling

It is important to model the dead volumes introduced by valves, connecting tubes and pumps. It is especially the case in experimental setup where some pumps, UV detectors,

capillaries replacing columns and long connectons are placed in the circulating loop between the columns. Normally, there are two options available here, continuous stirred tank reactor (CSTR) and dispersion plug flow reactor (DPFR).

If the CSTR strategy is used to characterize the dynamics of dead volume, it is modeled by the following equation:

$$\frac{\mathrm{d}c_i}{\mathrm{d}t} = \frac{c_i^{in}(t) - c_i^{out}(t)}{\tau} \tag{10}$$

where τ is the resident time in the continuous stirred tank reactor, and the c_i^{in} is the time-dependent concentration from the previous column. The solution of Eq.(10) can be easily obtained via employing the *ode* solver. The dead volume under DPFR situation is modeled by the one dimension convection-diffusion model:

$$\frac{\partial c_i}{\partial t} = -u^d \frac{\partial c_i}{\partial z} + D_{ax}^d \frac{\partial^2 c_i}{\partial z^2} \tag{11}$$

where the u^d is the interstitial velocity in the dead volume, and D_{ax}^d is the dispersion coefficient in the dead volume. And the commonly adopted boundary conditions is still the Danckwerts boundary conditions. The Eq.(11) is solved by the MATLAB *ode15s* routine after spatial discretization.

2.4 The Design of the Flow Rates and Switch Time

Under ideal situations, we can use triangle theory to design switching time and flow rates in order to separate components completely. We involve a brief introduction of triangle theory here without the derivation. Let us consider the model within the equilibrium, where axial dispersion D_{ax} is neglected and mass transfer resistances are considered negligible. Under those assumptions, we have the design criterion of the Henry coefficients and dimensionless flow-rate ratio to separate components completely.

$$\begin{cases} H_B \le m_{\mathrm{I}} \\ H_A \le m_{\mathrm{II}} \le H_B \\ H_A \le m_{\mathrm{III}} \le H_B \\ m_{\mathrm{V}} \le H_A \end{cases} \tag{12}$$

where m_k, the dimensionless flow-rate ratio of zone j, is defined as

$$m_k = \frac{Q_k t_s - V\varepsilon}{V(1-\varepsilon)} \qquad k = \mathrm{I}, \mathrm{II}, \mathrm{III}, \mathrm{IV}, \mathrm{V}. \tag{13}$$

Therefore, the following relationships are valid: $Q_{\mathrm{IV}} < Q_{\mathrm{II}} < Q_{\mathrm{III}} < Q_{\mathrm{I}}$. Similarly, Eq.(12) is able to be extended to ternary scenario (in default, $H_A < H_B < H_C$):

$$\begin{cases} H_C \le m_{\mathrm{I}} \\ H_B \le m_{\mathrm{II}} \le H_C \\ H_A \le m_{\mathrm{III}} \le H_B \\ H_A \le m_{\mathrm{IV}} \le H_B \\ m_{\mathrm{V}} \le H_A \end{cases} \tag{14}$$

However, due to the limitation of the triangle theory, modern algorithms are more preferable due to the published papers. And there are also different type of optimizers are accessible in the software, ranging from deterministic algorithm to heuristic algorithms to Bayesian inference.

3 CADET-SMB

3.1 Code Structure

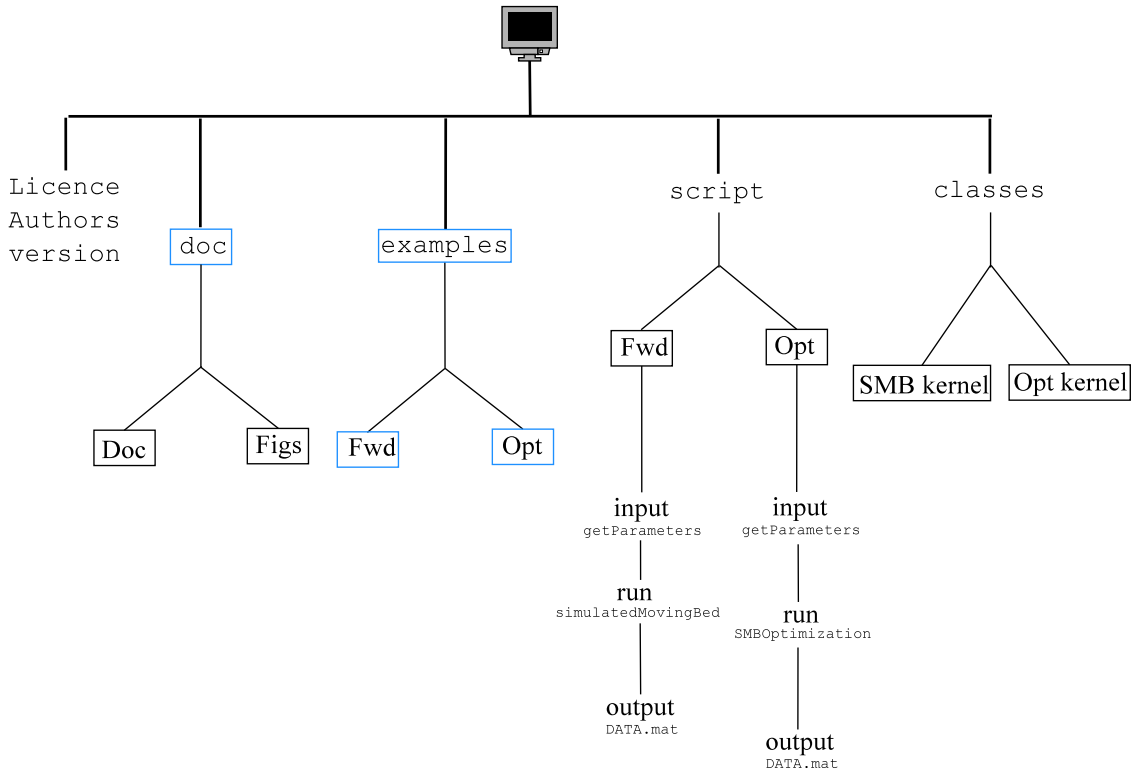

Figure 4: The code structure of the CADET-SMB

3.2 Switch Implementation

As for the switching, it is achieved by such a circle shifting: each zone is represented by alphabets, say, a, b, c, d (here we will simplify the presentation by considering the simple case when $N = 4$), and each column is sticked with Arabic numbers, 1, 2, 3, 4. Assuming the initial value assignment is $a = 4, b = 1, c = 2, d = 3$; then in the first switch interval, $a = 1, b = 2, c = 3, d = 4$, afterwards in the second switch interval, $a = 2, b = 3, c = 4, d = 1$.

3.3 Convergence Criterion

Until now all the essential conditions and operating parameters have been well-prepared, the simulations can be launched. First of all, what happens in a column during a switch interval is defined by the initial condition and the boundary condition. At the very beginning, the outlet of each columns is assumed to 0, $c_i^{out,j} = 0$. Then the four columns in the SMB unit are sequentially calculated, subsequently the data in demand (like outlets and the column state) are stored. Afterwards, the switch step is implemented. Using the mass conservation law to calculated the inlet concentration of each column and transferring the last state of column j in the former switch to the initial state of column $j+1$ in the next switch, the data for a simulation is ready again. The cyclic steady state (CSS) is reached once the following stopping criterion was satisfied:

$$\left|\left| \frac{\sum_{i=1}^{N_{comp}} [c_i(z, t + Nt_s) - c_i(z, t)]}{\sum_{i=1}^{N_{comp}} c_i(z, t)} \right|\right|_2 < \varepsilon \tag{15}$$

In the software, the value of 1×10^{-4} is enough for the relative error tolerance ε, and N is the column amount in the SMB unit. Regarding the choice of the tolerance accuracy, we have an explicit discussion in the numerical comparison section.

4 Demonstration of the Case 1

4.1 Case Data

The data for numerical tests (see Tab.(1)) were taken from a paper named *Numerical method for accelerated calculation of cyclic steady state of ModiCon-SMB-process*. But the particle radius was not provided in that paper, instead I just use a artificially empirical one.

The process needs around 80 switches to reach the so-called cyclic steady state (the relative tolerance $\varepsilon = 1 \times 10^{-4}$). The periodic concentration profiles along the SMB unit are shown in the following Fig.(5).

Let's have an insight into the process by sequence.

4.2 Concentration Profiles at the End of the First Switch t_s

At the beginning of the first period, all the columns are empty and the initial condition is $C_i^{out,j} = \{0\}$ for all the i and j. During the whole period, the feed is injected into the system through the feed node, at a constant composition. Since the switching time t_s is well-designed, so the concentration plateau of the component 1 enters into the Zone IV, while the concentration plateau of the component 2 does not.

Fig.(6) illustrates the outlet profile (we do not have the immediate concentration profile, instead we use outlet profile) in the column at the time immediately before the moment when the columns are switched.

Table 1: Parameters of *Case 1* for the numerical tests

Parameter type	Value
components	2
Column configuration	1-1-1-1
Number of columns	4
Dispersion coefficient	$u \times 10^{-24}$
Porosity	0.83
Column diameter	0.02 m
Column length	0.25 m
Particle radius	-
Switching time	$t_s = 180\ s$
Linear isotherms	$H_A = 5.72$ $H_B = 7.70$
Concentration of feed	0.55 g/l
Cyclic flow rate	$9.62 \times 10^{-7}\ m^3/s$
Feed flow rate	$0.98 \times 10^{-7}\ m^3/s$
Raffinate flow rate	$1.40 \times 10^{-7}\ m^3/s$
Desorbent flow rate	$1.96 \times 10^{-7}\ m^3/s$
Extract flow rate	$1.54 \times 10^{-7}\ m^3/s$

4.3 Concentration Profiles at the End of the Second Switch $2t_s$

At the beginning of the second period ($t_s + \delta t$), the feed and the draw-off points are switched simultaneously to their next positions in the direction of the liquid phase flow. The evolution of the concentration profiles during this period depends on the new initial and boundary conditions for each column. Specifically, the inlet concentration (initial boundary) of Zone II during this period is the outlet chromatogram in Zone III in previous period, while the inlet concentration of Zone III during this period is the combination of the outlet chromatogram in Zone IV in previous period and *feed concentration*. As a consequence, at the end of second period, we obtain such concentration profile Fig.(7) at the outlet of each column.

4.4 Profiles at the End of the Third Period $3t_s$

Again, the column switching at the beginning of the new period changes the initial conditions in the four columns and their boundary conditions. The inlet concentration (initial boundary) of Zone I during this period is the outlet chromatogram in Zone II in previous period, while the inlet concentration of Zone II during this period is the combination of the outlet chromatogram in Zone III in previous period and *feed concentration*, while the inlet concentration (initial boundary) of Zone III during this period is the outlet chromatogram in Zone IV in previous period. The calculation of the position of the concentration follows an iteration process. The concentration profiles in the SMB train, at the end of the third period, are shown in the Fig.(8).

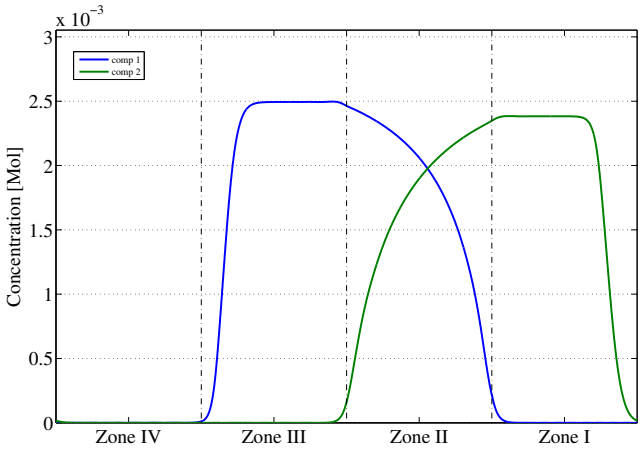

Figure 5: The concentration profiles of a four-column SMB unit for binary separation

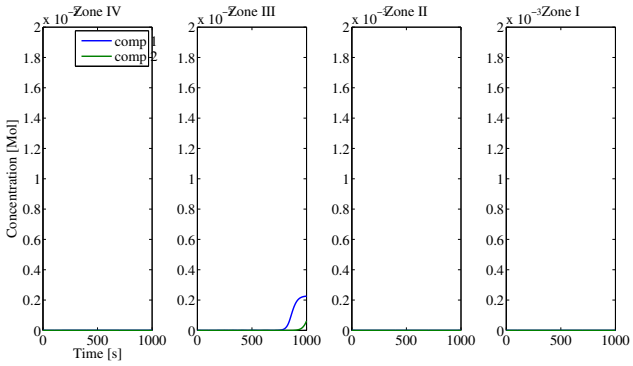

Figure 6: Concentration profiles along the column train of a SMB unit at the end of the first switch period. The plotted data are the outlet concentration of each columns. From right to left is the direction of the liquid phase, and from left to right is the switching direction of the columns.

4.5 Profiles at the End of the One Round $4t_s$

We define four switches as one round here. The iteration pattern is now clear. From one period to next, the higher and higher concentration plateaus are formed for components 1 and 2 in *Zone III*. These plateaus are transferred at the beginning of the following period into *Zone II*. These plateaus become narrower and narrower with increasing number of periods. Fig.(9) is the result of one round switching.

4.6 Profiles at the End of the nth Rounds nt_s

After several rounds, the iterative point approaches the convergence region. Fig.(10) and Fig.(11) are the concentration profiles of 3 cycles and 5 cycles respectively.

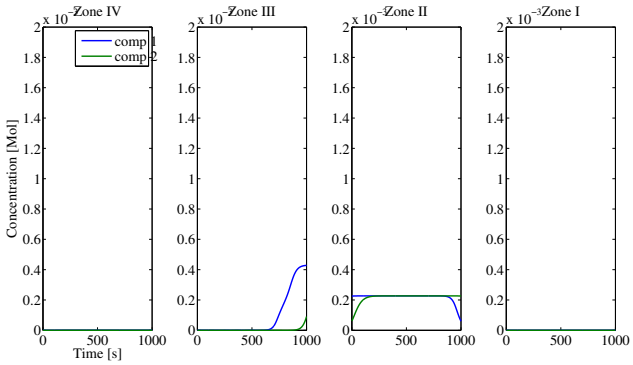

Figure 7: Concentration profiles at the end of the second period.

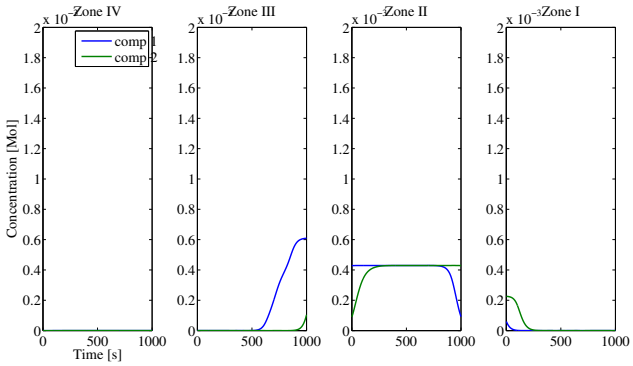

Figure 8: Concentration profiles at the end of the third period.

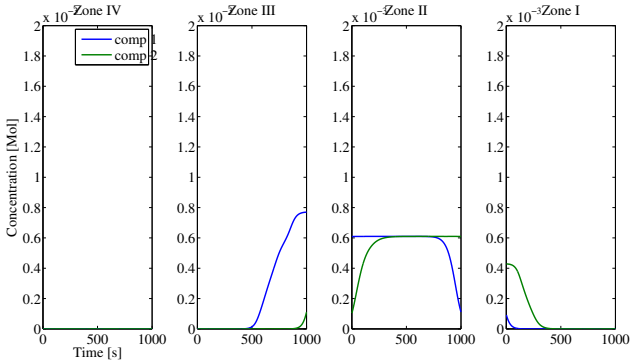

Figure 9: Concentration profiles at the end of the fourth period (one round).

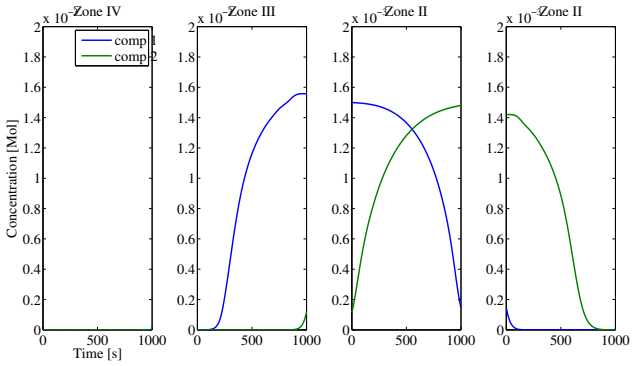

Figure 10: Concentration profiles at the end of the 3 cycles.

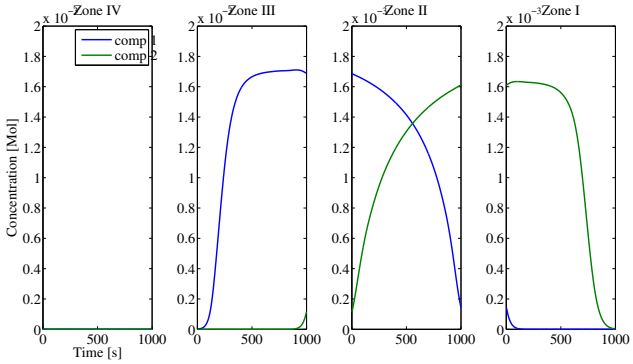

Figure 11: Concentration profiles at the end of the 5 cycles.

The above *Case 1* is a four-column case with one column in each Zone. Actually it can be extended into eight-column case once the parameter *opt.nColumn* was set to the value 8.

5 The Other Cases

The artificial data of a eight-column case (see Tab.(2)) was taken from the paper, *Model-based control of a simulated moving bed chromatographic process for the separation of fructose and glucose*.

Table 2: Parameters of *Case 2* for the numerical tests

Parameter type	Value
Components	2
Column configuration	2-2-2-2
Number of columns	8
Dispersion coefficient	3.8148×10^{-6}
Porosity	0.38
Column diameter	0.026 m
Column length	0.536 m
Particle radius	0.0016 m
Switching time	$t_s = 1552$ s
Linear isotherms	$H_A = 0.54$ $H_B = 0.28$
Concentration of feed	0.5 g/cm^3
Cyclic flow rate	0.1395×10^{-6} m^3/s
Feed flow rate	0.020×10^{-6} m^3/s
Raffinate flow rate	0.0266×10^{-6} m^3/s
Desorbent flow rate	0.0414×10^{-6} m^3/s
Extract flow rate	0.0348×10^{-6} m^3/s

The Fig.(12) is the concentration profile of the SMB fructose/glucose separation.

The monitored concentration profiles at the raffinate port and extract port are show in the Fig.(13)

The convergence to the cyclic steady state, in this eight-column case, is achieved after around 120 switching periods (300 sec), under the tolerance 1×10^{-5}. This result in approx. 140 sec on a 2.93GHz Intel Core i7 PC. In order to monitor each column, we plot the figures in terms of each column (by recording the outlet profiles of each column in one round), rather than the outlets in each switch period (such as the figures in demonstration of *Case 1*).

6 Summary

In this brief documentation, I intend to go through the fundamentals of the standard simulated moving bed (SMB) chromatographic process. It involves the mathematical models,

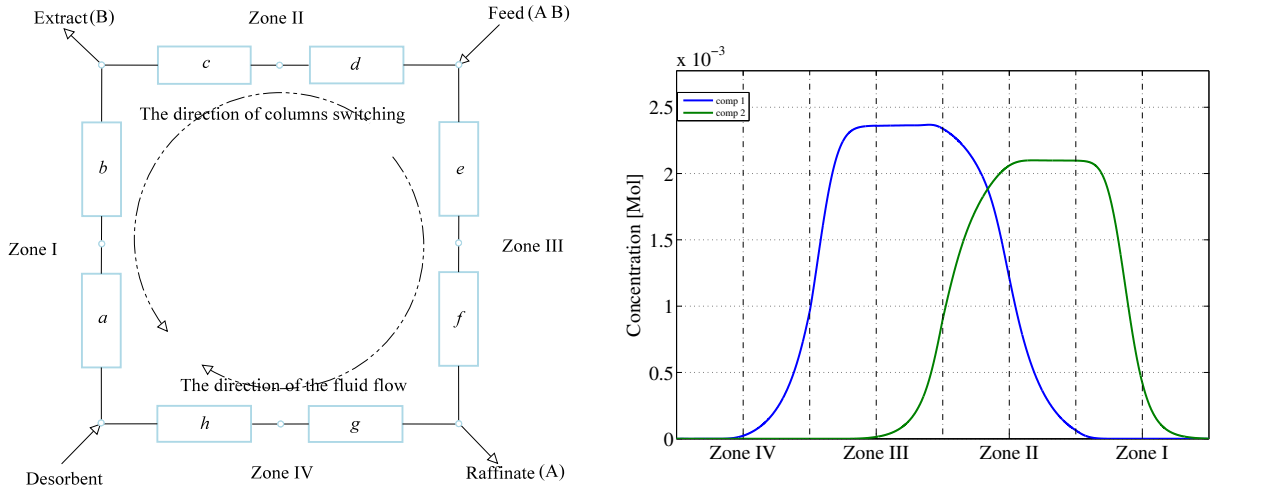

(a) The schematic of the eight-column SMB process

(b) The concentration profiles of the eight-column SMB for binary separation

Figure 12: The figures of the *Case 2*

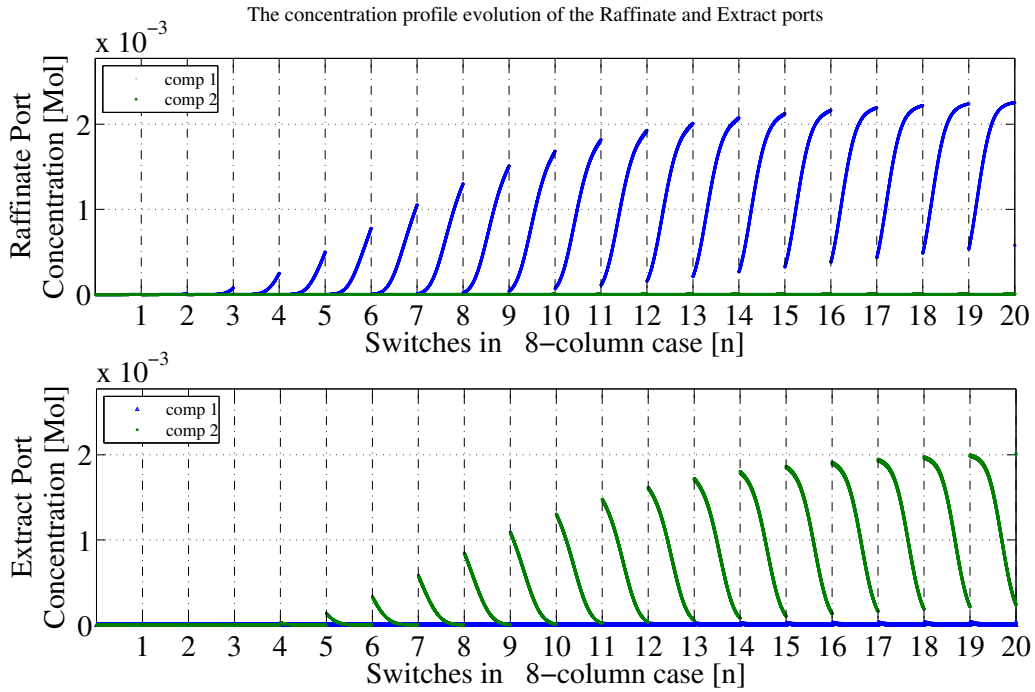

Figure 13: The monitored concentration profiles at the raffinate port and extranct port

CADET-SMB, cases demonstration.

In the mathematical modes part, the modelling that could be used in the CADET-SMB are all collected into this part, such as chromatography column modelling, node mass conservation, dead volumes modelling, and the designs of the flow rates and switch time. In the CADET-SMB section, some necessarily supplements are attached, like the diagram of the code structure, how to implement switch in the CADET-SMB, and lastly the stopping criterion. There are two cases are used to demonstrate the binary separation scenarios, one is a four-column case while another one is eight-column case. Notably, in the four-column case, a step-by-step illustration of the SMB process is provided.

Using CADET-SMB not only the concentration profile under cyclic steady state can be observed, but also the periodic profiles that monitored at the raffinate and extract ports can be observed. This is an introduction mainly for the standard SMB approach. As for more advanced and attractive approaches (e.g. one-column analog approach and operator-splitting approach), they are included in the respective *doc* directories.